DR. XIANGHUI FU (Orcid ID : 0000-0001-9808-3892)

Article type : Original

An Endoplasmic Reticulum Stress-MicroRNA-26a Feedback Circuit in Nonalcoholic Fatty Liver Disease

Haixia Xu[1,9], Yan Tian[1,9], Dongmei Tang[1], Sailan Zou[1], Geng Liu[1], Jiulin Song[2], Guixiang Zhang[3], Xiao Du[3], Wei Huang[4], Bin He[5], Weiqiang Lin[6], Liang Jin[7], Wendong Huang[8], Jiayin Yang[2,*], Xianghui Fu[1,*]

[1]Division of Endocrinology and Metabolism, State Key Laboratory of Biotherapy and Cancer Center, West China Hospital, Sichuan University and Collaborative Innovation Center of Biotherapy, Chengdu 610041, China.

[2]Department of Liver surgery, West China Hospital of Sichuan University, Chengdu 610041, Sichuan, China.

[3]Department of Gastrointestinal Surgery, Laboratory of Bariatric and Metabolic Surgery, West China Hospital, Sichuan University, Chengdu 610041, China.

[4]Department of Integrated Traditional Chinese and Western Medicine, Sichuan Provincial Pancreatitis Centre and West China-Liverpool Biomedical Research Centre, West China Hospital of Sichuan University, Chengdu 610041, China.

[5]Department of Emergency, West China Hospital, Sichuan University, Chengdu 610041, China

[6]The Fourth Affiliated Hospital, Institute of Translational Medicine, Zhejiang University School of Medicine, Hangzhou 310029, China

[7]State Key Laboratory of Natural Medicines, Jiangsu Key Laboratory of Druggability of Biopharmaceuticals, School of Life Science and Technology, China Pharmaceutical

University, Nanjing, China.

[8]Department of Diabetes Complications and Metabolism, Diabetes & Metabolism Research Institute of City of Hope, Beckman Research Institute of City of Hope, Duarte, CA 91010, USA.

[9]These authors contributed equally to this work.

*Correspondence to: Xianghui Fu (xfu@scu.edu.cn), Division of Endocrinology and Metabolism, State Key Laboratory of Biotherapy, West China Hospital, Sichuan University, Chengdu 610041, Sichuan, China; Jiayin Yang (doctoryjy@scu.edu.cn), Department of Liver surgery, West China Hospital of Sichuan University, Chengdu 610041, Sichuan, China.

Key words: Noncoding RNA, EIF2α, Lipid Metabolism, Insulin Resistance, Obesity

Electronic word count: Abstract: 240; Manuscript from introduction through references: 5950

Numbers of Figures and Tables: 8

List of Abbreviations

Ago2, argonaute RISC catalytic component 2; ATF6, activating transcription factor 6; BiP, binding-immunoglobulin protein; CHOP, C/EBP homologous protein; eIF2α, eukaryotic translation initiation factor 2 alpha; ER, Endoplasmic reticulum; HFD, high-fat diet; H&E, Hematoxylin-Eosin; IRE1α, inositol-required enzyme 1; miRNA, microRNA; NAFLD, nonalcoholic fatty liver disease; ORO, oil red O staining; PA, palmitate acid; PDI, protein disulfide isomerase; PERK, protein kinase R (PKR)-like endoplasmic reticulum kinase; QRT-PCR, quantitative real time polymerase chain reaction; RIP, RNA immunoprecipitation; siRNA, small interfering RNA; Tg, thapsigargin; Tu, tunicamycin; XBP1, X-box binding protein.

Financial Support

This work was supported by the Ministry of Science and Technology of China (2018ZX09201018-005), the National Natural Science Foundation of China (81570527, 81970561, 91540113, and 81502631), the National Cancer Institute of USA (NCI2R01CA139158), and the 1.3.5 Project for Disciplines of Excellence, West China Hospital, Sichuan University (ZYJC18049 and ZY2017308).

Potential conflict of interest

Nothing to report.

Abstract

Endoplasmic reticulum (ER) stress is an adaptive response to excessive ER demand and contributes to the development of numerous diseases, including nonalcoholic fatty liver disease (NAFLD) that is hallmarked by the accumulation of lipid within hepatocytes. However, the underlying mechanisms remain elusive. MicroRNAs (miRNAs) play an indispensable role in various stress responses, but their implications in ER stress have not yet been systemically investigated. In this study, we identify a negative feedback loop comprising hepatic ER stress and miR-26a in NAFLD pathogenesis. Combining miRNA dot blot array and quantitative polymerase chain reaction, we find that miR-26a is specifically induced by ER stress in liver cells. This induction of miR-26a is critical for cells to cope with ER stress. In human hepatoma cells and murine primary hepatocytes, overexpression of miR-26a markedly alleviates chemical-induced ER stress, as well as palmitate-triggered ER stress and lipid accumulation. Conversely, deficiency of miR-26a exhibits opposite effects. Mechanistically, miR-26a directly targets the eukaryotic initiation factor 2α (eIF2α), a core ER stress effector controlling cellular translation. Intriguingly, miR-26a is reduced in the livers of NAFLD patients. Hepatocyte-specific restoration of miR-26a in mice significantly mitigates high-fat diet (HFD)-induced ER stress and hepatic steatosis. In contrast, deficiency of miR-26a in mice exacerbates HFD-induced ER stress, lipid accumulation, inflammation and hepatic steatosis.

Conclusion: Our findings suggest ER stress-induced miR-26a upregulation as a regulator for hepatic ER stress resolution, and highlight the ER stress/miR-26a/eIF2α cascade as a promising therapeutic strategy for NAFLD.

Introduction

Nonalcoholic fatty liver disease (NAFLD) represents a spectrum of disorders ranging from simple steatosis to nonalcoholic steatohepatitis (NASH) and is characterized by excessive hepatic lipid accumulation (1). NAFLD may evolve into fibrosis, cirrhosis and ultimately progress to hepatocellular carcinoma (HCC). In addition, NAFLD is strongly associated with insulin resistance, obesity, type 2 diabetes (T2D) and cardiovascular diseases, thereby serving as an important component of metabolic complications. Due to its 20%-40% morbidity worldwide, NAFLD is becoming the leading cause of chronic liver diseases and has emerged as a serious public health issue (2, 3). Unfortunately, there are no efficacious pharmacological treatments for NAFLD (4), primarily due to our inadequate understanding of molecular mechanism underlying NAFLD pathogenesis. Therefore, it is urgent to identity novel therapeutic targets involved in the onset and progression of NAFLD.

Endoplasmic reticulum (ER) stress plays an important role in the pathogenesis of liver diseases including NAFLD, and thus ER stress-related molecules have becoming emerging therapeutic targets to treat these diseases (5). ER stress is primarily orchestrated by three ER-localized sensors, namely PKR-like ER kinase (PERK), inositol-required 1 (IRE1) and activating transcription factor 6 (ATF6), which coordinately decrease the load of unfolded proteins to restore organelle homeostasis. Particularly, PERK phosphorylates the α subunit of eukaryotic translation initiation factor 2 (eIF2α) at serine 51, which subsequently prevents the GDP/GTP exchange reaction and attenuates general protein translation, thereby relieving ER workload (6, 7). Impaired eIF2α phosphorylation disposes adult mice to obesity, insulin resistance and glucose intolerance (8). In contrast, selective inhibition of eIF2α dephosphorylation protects cells from ER stress (9-11). Although the ER stress response is a highly regulated process to restore the ER homeostasis, the excessive or prolonged ER stress is closely linked to various diseases, including NAFLD (12-14). Despite the close association of ER stress and NAFLD, the mechanism(s) underlying the dynamic regulation of ER stress is still poorly

understood.

Recently, microRNAs (miRNAs), a class of short (19–25 nt) and highly conserved noncoding RNAs that mainly mediate post-transcriptional gene silencing, have been implicated in the regulation of ER stress (15, 16). However, the interaction between ER stress and miRNAs in the pathogenesis of liver diseases is scarcely reported. For example, ER-stressed HCC cells can release increased exosomal miR-23a-3p, which subsequently promotes hepatocarcinogenesis through upregulating PD-L1 expression in macrophages (17). Specifically, although several miRNAs have been hinted in the network between ER stress and lipid dysregulation (18), the *in vivo* functions of these miRNAs in NAFLD are poorly understood. Moreover, no study systemically investigates the contribution of miRNAs to hepatic ER stress thus far.

MiR-26a is broadly expressed at high levels in human tissues and plays an important role in diverse biological and physiological processes (19-24). Particularly, we recently showed that hepatic miR-26a is significantly reduced in obese mice and overweight humans (21). Moreover, miR-26a can enhance insulin sensitivity and prevent obesity-associated metabolic abnormalities in the liver (21). More recently, it has indicated that miR-26a can potentially attenuate free fatty acid-induced hepatocyte injury *in vitro* (25). These data suggest a potential involvement of miR-26a in NAFLD pathogenesis, but the underlying mechanism remains largely unknown.

In this study, we report an ER stress-miR-26a feedback circuit in NAFLD. ER stress significantly induces the expression of miR-26a in liver cells. Conversely, miR-26a alleviates hepatic ER stress through targeting eIF2α. Administration of miR-26a remarkably modulates ER stress and lipid accumulation *in vitro* and *in vivo*. Moreover, components of the ER stress-miR-26a feedback loop are differentially expression in human NAFLD cohort relative to normal liver tissues. Overall, our data uncover a role of ER stress-miR-26a feedback loop in NAFLD pathogenesis and suggest miR-26a as a potential target for treating ER stress-associated liver diseases.

Materials and Methods

Clinical Specimens

Normal and NAFLD liver tissues were obtained from West China Hospital, Sichuan University. NAFLD is histologically diagnosed when steatosis occurs in > 5% hepatocytes. All procedures involving human liver samples were approved by the Ethics Committee of Sichuan University and conducted in accordance with the Declaration of Helsinki. Written informed consents were obtained from all subjects or from the family of the liver donor. Clinical sample information was shown in Supporting Table S1.

Animals

Generation of TG (CAG-Neo-STOP^{fl}-Mir26a1) mice, hepatocyte-specific miR-26a TG mice (Alb-TG), and miR-26a double knockout (26a DKO) mice have been previously described respectively (21, 24, 26) . Primers for genotyping are listed in Supporting Table S2.

All mice used in this study were on C57BL/6 background and maintained in specific pathogen-free (SPF) environment. 6-8-week-old male 26a DKO and wild type (WT) littermates were kept on high-fat diet (HFD) consisting of 60% kcal from fat (Research Diets) for 8 weeks to establish NAFLD mouse models. All mouse-based experiments were conducted according to the protocols approved by the Institutional Animal Care and Use Committee of Sichuan University.

Cell Culture and Murine Primary Hepatocytes

HepG2, Huh7, 786-O and HEK-293T cells were obtained from American Type Culture Collection. Normal human dermis fibroblasts (NHDF) were kindly provided by Dr. Jun Wu (City of Hope). Murine primary hepatocytes (MPHs) were isolated and cultured as described previously (27). For ER stress induction, cells were treated with tunicamycin (Tu), thapsigargin (Tg), A23187, palmitate acid (PA), or oleate acid (OA) for indicated times.

miRNA Dot Blot Array

Dot blot arrays were performed as described previously (28, 29). Briefly, miRNA array was

constructed by spotting antisense miRNA oligonucleotides on nylon membranes. Small RNAs were isolated from HepG2 cells using the *miRVana* Isolation Kit (Ambion). Then the 18- to 28-nucleotide RNA fraction was obtained, labeled and hybridized to the array. miRNAs examined in dot blot array are listed in Supporting Table S3.

***In vivo* Protein Synthesis Measurement**

The Surface Sensing of Translation (SUnSET) assay was performed to determine protein synthesis as described previously with minor modifications (30, 31). Briefly, Alb-TG mice and their WT littermates were fed a HFD for 5 days and intraperitoneally injected with puromycin (0.04 μmol/g body weight, MCE) in sterile saline. Thirty minutes post injection, liver tissues were collected for western blot using anti-puromycin antibody (1:15,000 dilution, Millipore). Puromycin incorporation into the newly synthesized peptides reflects the global protein synthesis rate.

RNA extraction and QRT-PCR

Total RNA extraction and quantitative real-time PCR (QRT-PCR) were performed as described previously (26). The primers for miRNAs were purchased from GenePharma (Shanghai, China). Primers for mRNAs are provided in Supporting Table S4.

Western Blotting

Western blot analysis were performed as described previously (32). Western blot antibodies are listed in Supporting Table S5.

Statistical Analysis

All data represent at least three independent experiments and are shown as means ± SEM. $P < 0.05$ was considered significant and indicated by $^{*}P < 0.05$, $^{**}P < 0.01$, $^{***}P < 0.001$. Analyses performed included two-way analysis of variance, Student *t* test, and paired *t* test where appropriate.

Additional materials and methods are described in the Supporting Information.

Results

MiR-26a Expression in Liver Cells Is Induced by Chemical-triggered ER Stress

To determine the potential association of miRNAs with ER stress in a systematic and comprehensive way, we first undertook an unbiased high-throughput screen of miRNAs in HepG2 cells treated with tunicamycin (Tu) or thapsigargin (Tg), using our previously developed dot blot array (29). A number of miRNAs were differentially expressed after Tu or Tg treatment (Fig. 1A and Supporting Fig. S1), suggesting a broad effect of ER stress on miRNA expression. Then we examined the expression of these miRNAs in response to ER stress by QRT-PCR analysis. It confirmed that four miRNAs, namely miR-29a, miR-26a, miR-194 and miR-22, were significantly induced by Tu treatment (Fig. 1B and Supporting Table S6). In line with our results, miR-29a has been recently shown to be increased by ER stress in neurons (33). Moreover, we determined the expression of these four miRNAs in response to distinct ER stressors in HepG2 cells. QRT-PCR analysis revealed miR-26a as the only miRNA for which expression was markedly induced by all three ER stressors (Tu, Tg and A23187) (Fig. 1C), which induce ER stress by distinct mechanisms. Therefore, we chose miR-26a for further analysis and examined its expression in additional cell lines. QRT-PCR analysis showed that miR-26a was also induced by ER stress in another hepatoma cell line Huh7, and in murine primary hepatocytes (MPHs), but not in the kidney cell line 786-O (Fig. 1D,E). In addition, we determined the expression of miR-26a in response to palmitate acids (PA) and oleate acids (OA) that are representative fatty acids for triggering ER stress. Both PA and OA markedly induced miR-26a expression in MPHs and Huh7 cells (Fig. 1F,G). Together, these results suggest miR-26a as a specific miRNA induced by ER stress in liver cells.

MiR-26a Alleviates ER Stress in Liver Cells

We then explored the biological implications of miR-26a induction in ER stress. To this end, HepG2 cells were transfected with miR-26a mimics, followed by Tu or Tg treatment for 24 hours. Western blot analyses showed that the levels of ER stress

markers, including p-eIF2α, IRE1α, and CHOP, were markedly reduced in miR-26a-overexpressing cells (Fig. 2A and Supporting Fig. S2A). Similar effect of miR-26a on ER stress was observed in HepG2 cells by different doses of Tu treatment for 24 hours (Fig. 2B and Supporting Fig. S2B). Moreover, the inhibition of miR-26a overexpression on ER stress markers was recapitulated in HepG2 cells after short-term Tu treatment (Fig. 2C and Supporting Fig. S2C).

Interestingly, miR-26a-overexpressing cells exhibited an obvious decrease in total eIF2α proteins (Fig. 2A-C). Previous studies have centered on the physiological roles of phosphorylation of eIF2α (7, 8), while the effect of total eIF2α remains poorly understood. Therefore, we silenced eIF2α by siRNAs in HepG2 cells and found eIF2α knockdown led to a similar expression pattern of ER stress markers as that of miR-26a overexpression (Fig. 2D and Supporting Fig. S2D), suggesting a robust effect of miR-26a on ER stress and a possible association between miR-26a and eIF2α. Accordingly, mRNA expression of ER stress markers, including Bip, Chop and Hepcidin, was suppressed by miR-26a overexpression at 5 hours post Tu treatment (Fig. 2E). Taken together, these results suggest that ER stress-induced miR-26a upregulation may accelerate liver cells recovery from experimental ER stress.

MiR-26a Directly Targets EIF2α

To investigate the molecular mechanism(s) underlying the function of miR-26a in ER stress, we attempted to identify the potential target of miR-26a. Eif2s1 that encodes eIF2α，was the top candidate target of miR-26a in the ER stress pathway, as predicted by TargetScan (34). Among numerous Eif2s1-regulating miRNAs, miR-26a was ranked as the most potential candidate for both human and murine Eif2s1 (Supporting Table S7 and S8). Notably, human Eif2s1 contains five putative miR-26a binding sites, and two of them are preferentially located near both ends of its 3'-UTR (Fig. 3A and Supporting Fig. S3A), implying effective targeting (35). Murine Eif2s1 has two putative miR-26a binding sites (Fig. 3A and Supporting Fig. S3B). Moreover, this putative regulation is also present in

zebrafish (Supporting Fig. S3C), which is consistent with the emergence of miR-26a during evolution (24) and thus suggests strong conservation.

To determine whether miR-26a directly targets Eif2s1 through its 3'UTR, we cloned fragments of the human Eif2s1 3'UTR and created two luciferase reporter constructs: hEif2s1-1 and hEif2s1-2. hEif2s1-1 contained four predicted miR-26a binding sites, while hEif2s1-2 contained one site. MiR-26a strongly repressed hEif2s1 3'UTR activity in both constructs (Fig. 3B). Moreover, mutations in the seed sequence of the predicted miR-26a binding sites abolished the inhibitory effects of miR-26 (Fig. 3B), suggesting a direct targeting of miR-26a on human Eif2s1. Similar luciferase reporter assays showed that miR-26a can directly target murine Eif2s1, primarily through the binding site 2 (Supporting Fig. S4).

The mouse and human genomes contain two miR-26a loci (miR-26a-1 and miR-26a-2) that generate identical mature miR-26a, implying a potential functional redundancy. To overcome this redundancy, we have generated miR-26a double knockout (26a DKO) lacking both miR-26a-1 and miR-26a-2 locus (26) (Supporting Fig. S5A). As expected, the expression of miR-26a was abolished in 26a DKO mice (Supporting Fig. S5B). To further verify the direct interaction between miR-26a and Eif2s1 *in vivo*, we performed Ago2 RIP analysis in the livers from 26a DKO mice and their WT littermate controls. Similar as the known miR-26a target Cd36, Eif2s1 was significantly enriched in the Ago2 RIP fraction from WT mice compared with 26a DKO mice, while the negative control Gapdh was comparable in both genotypes (Fig. 3C).

We next determined the effect of miR-26a on eIF2α expression. Overexpression of miR-26a resulted in a decrease in eIF2α protein expression in human cell lines (Fig. 3D). By using our recently established liver-specific miR-26a transgenic mice (Alb-TG) (21), we found that the level of eIF2α protein was markedly decreased in the livers of Alb-TG mice compared with that of WT littermate controls (Fig. 3E). EIF2α is essential for global protein synthesis, we thus tested the consequence of miR-26a overexpression on protein synthesis. [^{35}S] metabolic labeling analysis revealed that HepG2 cells post Tg treatment

for 6 hours exhibited a significant decrease in protein synthesis (Fig. 3F). However, miR-26a overexpression decreased basal protein synthesis and efficiently prevented the reduction of protein synthesis triggered by ER stress (Fig. 3F). To further verify the effect of miR-26a on hepatic protein synthesis *in vivo*, we utilized surface sensing of translation (SUnSET), a method that can monitor and quantify new protein synthesis in mammalian cells and tissues (30, 31). It showed that protein synthesis was lower in the livers of HFD-feeding Alb-TG mice than that of their WT littermates (Fig. 3G). These results collectively suggest that eIF2α is a direct target of miR-26a and the effect of miR-26a on ER stress may occur, at least in part, through eIF2α regulation.

Overexpression of MiR-26a in Mice Alleviates Obesity-induced ER Stress

ER stress plays a crucial role in the pathogenesis of NAFLD. We recently showed that global or hepatocyte-specific overexpression of miR-26a in mice significantly prevented obesity-induced insulin resistance (21). Given that the close association among ER stress, insulin resistance and lipid accumulation, we hypothesized that miR-26a may have a role in the development of NAFLD through modulating ER stress. In line with this notion, Alb-TG mice fed a HFD had lower levels of ALT and AST than WT control littermates (Fig. 4A and Supporting Fig. S6A), indicating a decreased liver injury in Alb-TG mice. More importantly, hepatic ER stress indicators, including p-eIF2α, p-PERK, BiP, CHOP and PDI, were all reduced in Alb-TG mice compared with WT littermates fed a HFD (Fig. 4B). mRNA levels of Bip and Chop were also significantly lower in Alb-TG mice than WT controls fed a HFD, as were mRNA levels of total and spliced Xbp1, a key regulator of ER stress (Fig. 4C and Supporting Fig. S6B). A slight, but not significant repression of ER stress was observed in the fat tissue of Alb-TG mice compared with WT controls (Supporting Fig. S6C). No difference of ER stress was found in the muscle of both genotypes (Supporting Fig. S6C), consistent with the previous observation that muscle is not associated with obesity-induced ER stress (12). Furthermore, we verified the protective role of miR-26a in liver cell injury *in vitro* and determined the contribution of

eIF2α in this function. To this end, we transiently overexpressed eIF2α in primary hepatocytes isolated from Alb-TG mice and WT littermate controls respectively, which were subsequently treated with PA. TUNEL assay showed that miR-26a overexpression significantly prevented PA-induced cell death, while eIF2α restoration markedly abolished this inhibitory effect (Supporting Fig. S7), indicating that eIF2α may contribute to the role of miR-26a in liver injury.

Accumulating evidence demonstrate that ER stress can lead to inflammation and the deregulation of lipid metabolism (5). Because we have already showed a potent regulation of miR-26a overexpression in numerous regulators of hepatic lipid metabolism (21), here we thus determined its consequences on inflammation. Alb-TG mice exhibited decreased expression of inflammatory genes (Il-1β, Il-6, Mcp1 and Tnfα) when compared with their WT littermates (Fig. 4D). Obesity-induced ER stress can activate JNK, which subsequently enhances Ser^{307} phosphorylation of IRS-1 and promotes insulin resistance (36). Indeed, JNK activity (p-c-Jun) was also markedly decreased in Alb-TG mice compared with WT littermates (Supporting Fig. S8). Furthermore, a cell-intrinsic alleviation in Tg-induced ER stress was confirmed in primary hepatocytes from Alb-TG mice (Fig. 4E). Taken together, these data indicate that miR-26a overexpression ameliorates obesity-induced hepatic ER stress *in vivo*.

Deficiency of MiR-26a Aggravates Chemical-induced ER stress in Liver Cells

We next determined the effect of miR-26a deficiency on ER stress *in vitro*. Primary hepatocytes isolated from 26a DKO mice and their WT littermates were treated with Tu for 12 and 24 hours, respectively. MiR-26a-deficient hepatocytes exhibited an increase in the protein levels of ER stress markers, such as p-eIF2α, BiP and IRE1α (Fig. 5A and Supporting Fig. S9A). We also measured the mRNA levels of Bip, Chop, and sXbp1 by QRT-PCR analysis and found that these genes were significantly upregulated in miR-26a-deficient cells compared with WT hepatocytes (Fig. 5B). Similar results were observed in MPHs treated with another ER stress inducer Tg (Fig. 5C,D and Supporting

Fig. S9B). Notably, the levels of total eIF2α proteins were markedly elevated in miR-26a-deficient hepatocytes, further supporting the targeting of eIF2α by miR-26a. Moreover, eIF2α knockdown markedly alleviated Tu-induced ER stress in primary hepatocytes isolated from 26a DKO mice (Fig. 5E). Collectively, these results suggest that miR-26a deficiency can deteriorate chemical-induced ER stress in liver cells.

Deficiency of MiR-26a in Mice Exacerbates Obesity-induced ER Stress and NAFLD

By using miR-26a DKO mouse line, we further evaluated the *in vivo* effect of miR-26a deficiency in obesity-induced ER stress and NAFLD. When 6- to 8-week-old mice were fed a HFD, 26a DKO mice exhibited higher body weights than WT littermate controls (Fig. 6A). After 8 weeks of HFD feeding, 26a DKO mice had increased AST and ALT levels compared with WT littermate controls (Fig. 6B). Liver histology, H&E and ORO staining analysis showed an elevated lipid accumulation in the livers of 26a DKO mice fed a HFD (Fig. 6C-E), although no obvious differences were detected between aged-matched 26a DKO mice and WT littermates fed a chow diet (Supporting Fig. S10). Consistently, the hepatic triglyceride and cholesterol levels were significantly higher in 26a DKO mice than in WT littermate controls (Fig. 6F). Plasma triglyceride, cholesterol, LDL and HDL concentrations in 26a DKO mice were also increased (Fig. 6G and Supporting Fig. S11A,B).

In line with the worsen phenotypes, 26a DKO mice fed a HFD had elevated ER stress, as evidenced by increased levels of p-eIF2α, CHOP and PDI (Fig. 6H). The mRNA levels of ER stress markers were also significantly upregulated in the livers of 26a DKO mice compared with WT controls (Fig. 6I). In accordance with the important role of ER stress in hepatic lipid metabolism, expression of several critical genes controlling fatty acid synthesis and oxidation, including Acc1, Acc2, Acly, Fasn, Lipc, and Scd1, were significantly increased in the livers of 26a DKO mice (Fig. 6I). Cd36 and Ldlr, two key regulators of cholesterol metabolism, were markedly increased in 26a DKO mice (Fig. 6I). In addition, ER stress is associated with chronic low-grade inflammation, which

contributes to the development of NAFLD. Indeed, the mRNA levels of inflammatory genes, including Il-1β, Il-6, Mcp1 and Tnfα, were higher in the livers of 26a DKO mice than that of WT littermate controls (Fig. 6I). These results collectively suggest that miR-26a deficiency in mice aggravates HFD-induced ER stress and hepatic steatosis.

NAFLD varies in severity from simple hepatic steatosis to NASH that is often characterized by fibrosis. Therefore, we tested the potential outcome of miR-26a deficiency in hepatic fibrosis. QRT-PCR and western bolts analysis showed expressions of the fibrotic markers were comparable in 26a DKO mice and their WT littermate controls fed a HFD for 8 weeks (Supporting Fig. S12A,B). Meanwhile, no obvious collagen deposition was seen in the livers of both genotypes, as evidenced by Masson's Trichrome staining (Supporting Fig. S12C). These observations are consistent with some recent concepts that short-term HFD feeding cannot lead to fibrosis and NASH (37, 38). It is interesting to clarify the role of miR-26a in fibrosis and NASH by using appropriate mouse models in the future.

MiR-26a Alleviates Palmitate-induced ER Stress and Lipid Accumulation

To further confirm our above findings, we investigated the effect of miR-26a on palmitate-induced hepatic ER stress *in vitro*. To this end, MPHs were isolated from 26a DKO mice and their WT littermates respectively, and then treated with PA. ORO staining showed that PA exposure for 24 hours led to a significant accumulation of lipids in MPHs (Fig. 7A). Notably, deficiency of miR-26a in MPHs markedly increased PA-induced lipid accumulation (Fig. 7A). Expression of ER stress-related molecules were further measured in MPHs after exposure to PA. Western blot analyses showed that the protein levels of p-eIF2α, eIF2α, BiP, and PDI were higher in MPHs from 26a DKO mice than that of WT controls (Fig. 7B). Consistently, the mRNA levels of ER stress markers, including Bip, Chop and sXbp1, were significantly upregulated in 26a DKO MPHs (Fig. 7C). Additionally, QRT-PCR analyses revealed that miR-26a deficiency remarkably increased the expression of regulators modulating hepatic lipogenesis (Acc2, Scd1), fatty acid oxidation

(Acox1, Cpt1α), fatty acid uptake (Plin2), and cholesterol synthesis (Hmgcr) (Fig. 7D). Strikingly, restoration of miR-26a expression in MPHs from 26a DKO mice significantly attenuated PA-induced ER stress and lipid accumulation (Fig. 7E-G). Taken together, these data further support a role of miR-26a in ER stress and lipid accumulation *in vitro*.

ER Stress/MiR-26a Regulatory Axis in Human NAFLD

We finally linked the relevance of our experimental findings on ER stress/miR-26a axis to NAFLD patients. MiR-26a levels were significantly reduced in the livers of NAFLD patients compared with that of non-steatosis individuals (Fig. 8A). Intriguingly, the host genes of miR-26-1 and miR-26a-2, namely Ctdspl and Ctdsp2 (Fig. 8B), as well as the primary transcripts and precursors of miR-26a (Fig. 8C,D), were unchanged, indicating a post-transcriptional regulation. The levels of ER stress markers, including Atf6, Bip, Chop and Eif2s1, were higher in the livers of NAFLD subjects than that of non-steatosis individuals (Fig. 8E). Moreover, western blot analyses showed that the protein levels of ER stress markers, such as p-eIF2α, eIF2α and PDI, were remarkably upregulated in the livers of NAFLD patients (Fig. 8F). These results suggest that the ER stress/miR-26a regulatory axis exists in human NAFLD.

Discussion

In this study, we identify an ER stress-miRNA functional circuitry that likely underlies the pathogenesis of NAFLD. In liver cells, miR-26a expression is induced by ER stress, and this, in turn, alleviates ER stress by targeting eIF2α. We demonstrate that overexpression of miR-26a ameliorates ER stress and lipid accumulation both *in vitro* and *in vivo*. Conversely, deficiency of miR-26a aggravates ER stress and NAFLD progression. Moreover, miR-26a is downregulated in human NAFLD livers, which is accompanied with increased expression of ER stress markers. Our findings thus reveal a crucial role of the ER stress-miR-26a feedback circuit in NAFLD pathogenesis (Fig. 8G) and suggest that manipulating miR-26a expression could provide potential opportunities for treating NAFLD.

NAFLD is hallmarked by the hepatic accumulation of lipids. The ER is the major site of lipid synthesis and a central function of ER stress response is to maintain hepatic lipid homeostasis, and thus increasing evidence suggests an important role of ER stress in the etiology of NAFLD. However, the interplay between ER stress and miRNAs that act as prominent regulators of stress responses (39, 40) has not been systemically investigated. Moreover, although certain miRNAs have been shown to interact with ER stress (16, 18), their implications in NAFLD have not yet determined. For example, ER stress can induce the expression of miR-30c-2-3p, which targets Xbp1 and thus promotes cell survival in the adaptive ER stress (41), but the pathological role of this axis remains unknown. In the present study, we performed a high-throughput screening of miRNA expression in ER-stressed HepG2 cells and identified miR-26a as the unique miRNA that can be stimulated by distinct ER stress inducers in hepatic cells. More strikingly, miR-26a can subsequently function as a negative feedback regulator of ER stress. Overexpression of miR-26a mitigated chemical-induced ER stress *in vitro*, whereas knockout of miR-26a exhibited opposite outcomes. Furthermore, miR-26a was reduced in the livers of obese mice (21) and human NAFLD patients. Restoration of miR-26a in mice reduced ER stress and NAFLD burden under obese conditions. Conversely, deficiency of miR-26a in mice

exasperated HFD-induced ER stress and promoted NAFLD progression. These results strongly suggest that the ER stress/miR-26a negative feedback loop is associated with the pathogenesis of NAFLD.

Mechanistically, we found that miR-26a directly targets the translation initiation factor eIF2α. eIF2α, the major substrate of PERK, is central to the rapid repression of global translation in response to ER stress. Importantly, miR-26a-mediated targets in the 3'-UTR of Eif2s1 is highly conserved among vertebrates, consistent with the observation that miR-26a is a vertebrate-specific miRNA. Thus, we speculated that the miR-26a/eIF2α regulatory axis might exert a broad, evolutionarily conserved role in development and disease. Given the significance of eIF2α in ER stress and protein synthesis, the dynamic regulation of its phosphorylation and dephosphorylation has been extensively studied, and pharmacological compounds targeting this phosphorylation-dephosphorylation cycle, such as salubrinal and guanabenz, have been explored in the context of NAFLD/NASH (18). In this regard, our study identifies a novel post-transcriptional regulatory mechanism of eIF2α expression and eventually offers new potential options for ER stress-associated diseases.

Three miRNAs, namely miR-122, miR-34a and miR-30, have been shown to interact with ER stress and have a potential to affect the development and progression of NAFLD (18). In addition to modulating ER stress, these three miRNAs can simultaneously control other pathways contributing to hepatic steatosis, thereby coordinately contributing to NAFLD pathogenesis. For instance, miR-122, the most enriched hepatic miRNA, is downregulated in the hepatic tissues of NAFLD/NASH patients. MiR-122 can regulate various pathways, such as ER stress, fatty acids synthesis and uptake, fatty acid oxidation, glycolysis, and glycogen metabolism, thus plays an important role in NAFLD and its progression to more severe stages. Notably, we previously showed that hepatic miR-26a targets several regulators crucial for lipid metabolism (Acsl3 and Acsl4), gluconeogenesis (Pck1 and Tcf7l2), and insulin signaling (Gsk3β, Pkcδ and Pkcθ), thereby preventing insulin resistance, elevated glucose production, and abnormal metabolism of lipids and

cholesterol under diabetic conditions (21). We also found that miR-26a could enhance autophagy and thus prevent ethanol-induced acute liver injury (22). In addition, a recent study suggests that miR-26a may attenuate the development of NAFLD via an immune-regulatory axis comprising IL-6 and IL-17 (42). Therefore, it is likely that the multifunctional roles of miR-26a act cooperatively to prevent NAFLD. The integrative transcriptomics, proteomics, epigenomics and genetics analysis approach are required to explore this possibility in the future.

We have demonstrated that miR-26a is induced by ER stress in both human hepatoma cells and MPHs. Given the existence of ER stress in NAFLD, we presumed an increase in miR-26a expression in the liver tissues of NAFLD patients. Unexpectedly, hepatic miR-26a was reduced in NAFLD patients compared with non-steatosis individuals, whereas expression of miR-26a host genes Ctdspl and Ctdsp2 was comparable in both cohorts. Interestingly, similar expression patterns of miR-26a and its host genes were seen in the livers of obese mice and overweight human, as we shown previously (21). These observations strongly suggest that miR-26a could be repressed at the post-transcriptional level during obesity, which results in antagonism of the inducible effect of ER stress and perturbation of the ER stress-miR-26a feedback circuit, thereby contributing to NAFLD development and progression. Indeed, recent studies have shown that miR-26a can be regulated at the post-transcriptional level by several mechanisms, including uridylation (43), A-I editing (44), and RNA G-quadruplex (RG4) (45). On top of these, we have recently revealed that a guanine-rich sequence within pre-miR-26a molecules can fold into RG4 and subsequently impair miR-26a biogenesis. Moreover, DHX36 that binds and unwinds this RG4 is reduced in obese mouse livers, further supporting our explanation for the reduction of miR-26a in NAFLD livers. It is of interest for future studies to investigate the mechanism underlying the post-transcriptional regulation of miR-26a in the development of NAFLD. Beyond this, the distinct pattern of miR-26a expression in liver cells *in vitro* and liver tissues *in vivo* under ER stress conditions might be also associated with other factors, such as difference between acute and chronic ER

stress, the multiple roles of HFD beyond ER stress, the complex hepatic ecosystem with various intercellular crosstalk, etc., which warrant future studies.

In conclusion, we reveal that an ER stress/miR-26a feedback circuitry is associated with the pathogenesis of NAFLD. Our findings suggest a novel miRNA-mediated approach to treat ER stress-associated liver diseases, including NAFLD.

References

1. Sanyal AJ. Past, present and future perspectives in nonalcoholic fatty liver disease. Nat Rev Gastroenterol Hepatol 2019;16:377-386.

2. **Zhou F**, **Zhou J**, **Wang W**, Zhang XJ, Ji YX, Zhang P, et al. Unexpected Rapid Increase in the Burden of NAFLD in China From 2008 to 2018: A Systematic Review and Meta-Analysis. Hepatology 2019;70:1119-1133.

3. Younossi Z, Tacke F, Arrese M, Chander Sharma B, Mostafa I, Bugianesi E, et al. Global Perspectives on Nonalcoholic Fatty Liver Disease and Nonalcoholic Steatohepatitis. Hepatology 2019;69:2672-2682.

4. Chen Z, Yu Y, Cai J, Li H. Emerging Molecular Targets for Treatment of Nonalcoholic Fatty Liver Disease. Trends Endocrinol Metab 2019;30:903-914.

5. Lebeaupin C, Vallee D, Hazari Y, Hetz C, Chevet E, Bailly-Maitre B. Endoplasmic reticulum stress signalling and the pathogenesis of non-alcoholic fatty liver disease. J Hepatol 2018;69:927-947.

6. Kimball SR. Eukaryotic initiation factor eIF2. Int J Biochem Cell Biol 1999;31:25-29.

7. Moon SL, Sonenberg N, Parker R. Neuronal Regulation of eIF2alpha Function in Health and Neurological Disorders. Trends Mol Med 2018;24:575-589.

8. Scheuner D, Song B, McEwen E, Liu C, Laybutt R, Gillespie P, et al. Translational control is required for the unfolded protein response and in vivo glucose homeostasis. Mol Cell 2001;7:1165-1176.

9. Boyce M, Bryant KF, Jousse C, Long K, Harding HP, Scheuner D, et al. A selective inhibitor of eIF2alpha dephosphorylation protects cells from ER stress. Science 2005;307:935-939.

10. Tsaytler P, Harding HP, Ron D, Bertolotti A. Selective inhibition of a regulatory subunit of protein phosphatase 1 restores proteostasis. Science;332:91-94.

11. Ozcan U, Yilmaz E, Ozcan L, Furuhashi M, Vaillancourt E, Smith RO, et al. Chemical chaperones reduce ER stress and restore glucose homeostasis in a mouse model of type 2 diabetes. Science 2006;313:1137-1140.

12. **Ozcan U**, **Cao Q**, Yilmaz E, Lee AH, Iwakoshi NN, Ozdelen E, et al. Endoplasmic reticulum stress links obesity, insulin action, and type 2 diabetes. Science 2004;306:457-461.

13. **Yang L**, **Li P**, Fu S, Calay ES, Hotamisligil GS. Defective hepatic autophagy in obesity promotes ER stress and causes insulin resistance. Cell Metab;11:467-478.

14. Zhang K, Kaufman RJ. From endoplasmic-reticulum stress to the inflammatory response. Nature

2008;454:455-462.

15. Tian Y, Xu J, Du X, Fu X. The interplay between noncoding RNAs and insulin in diabetes. Cancer Lett 2018;419:53-63.

16. McMahon M, Samali A, Chevet E. Regulation of the unfolded protein response by noncoding RNA. Am J Physiol Cell Physiol 2017;313:C243-C254.

17. **Liu J**, **Fan L**, **Yu H**, **Zhang J**, He Y, Feng D, et al. Endoplasmic Reticulum Stress Causes Liver Cancer Cells to Release Exosomal miR-23a-3p and Up-regulate Programmed Death Ligand 1 Expression in Macrophages. Hepatology 2019;70:241-258.

18. Gjorgjieva M, Sobolewski C, Dolicka D, Correia de Sousa M, Foti M. miRNAs and NAFLD: from pathophysiology to therapy. Gut 2019;68:2065-2079.

19. Li X, Pan X, Fu X, Yang Y, Chen J, Lin W. MicroRNA-26a: An Emerging Regulator of Renal Biology and Disease. Kidney Blood Press Res 2019;44:287-297.

20. Fu X, Meng Z, Liang W, Tian Y, Wang X, Han W, et al. miR-26a enhances miRNA biogenesis by targeting Lin28B and Zcchc11 to suppress tumor growth and metastasis. Oncogene 2014;33:4296-4306.

21. Fu X, Dong B, Tian Y, Lefebvre P, Meng Z, Wang X, et al. MicroRNA-26a regulates insulin sensitivity and metabolism of glucose and lipids. J Clin Invest 2015;125:2497-2509.

22. **Han W**, **Fu X**, Xie J, Meng Z, Gu Y, Wang X, et al. MiR-26a enhances autophagy to protect against ethanol-induced acute liver injury. J Mol Med (Berl) 2015;93:1045-1055.

23. Chen X, Xu H, Ding L, Lou G, Liu Y, Yao Y, et al. Identification of miR-26a as a target gene of bile acid receptor GPBAR-1/TGR5. PLoS One 2015;10:e0131294.

24. **Fu X**, **Jin L**, Wang X, Luo A, Hu J, Zheng X, et al. MicroRNA-26a targets ten eleven translocation enzymes and is regulated during pancreatic cell differentiation. Proc Natl Acad Sci U S A 2013;110:17892-17897.

25. Ali O, Darwish HA, Eldeib KM, Abdel Azim SA. miR-26a Potentially Contributes to the Regulation of Fatty Acid and Sterol Metabolism In Vitro Human HepG2 Cell Model of Nonalcoholic Fatty Liver Disease. Oxid Med Cell Longev 2018;2018:8515343.

26. **Xu H**, **Du X**, **Xu J**, Zhang Y, Tian Y, Liu G, et al. Pancreatic β cell microRNA-26a alleviates type 2 diabetes by improving peripheral insulin sensitivity and preserving β cell function. PLoS Biol 2020;18:e3000603.

27. **Xu H**, **Du X**, Liu G, Huang S, Du W, Zou S, et al. The pseudokinase MLKL regulates hepatic insulin sensitivity

independently of inflammation. Mol Metab 2019;23:14-23.

28. Fu X, Adamski M, Thompson EM. Altered miRNA repertoire in the simplified chordate, Oikopleura dioica. Mol Biol Evol 2008;25:1067-1080.

29. **Meng Z**, **Fu X**, Chen X, Zeng S, Tian Y, Jove R, et al. miR-194 is a marker of hepatic epithelial cells and suppresses metastasis of liver cancer cells in mice. Hepatology 2010;52:2148-2157.

30. Schmidt EK, Clavarino G, Ceppi M, Pierre P. SUnSET, a nonradioactive method to monitor protein synthesis. Nat Methods 2009;6:275-277.

31. Lipton JO, Yuan ED, Boyle LM, Ebrahimi-Fakhari D, Kwiatkowski E, Nathan A, et al. The Circadian Protein BMAL1 Regulates Translation in Response to S6K1-Mediated Phosphorylation. Cell 2015;161:1138-1151.

32. **Ma M**, **Xu H**, **Liu G**, **Wu J**, Li C, Wang X, et al. Metabolism-induced tumor activator 1 (MITA1), an Energy Stress-Inducible Long Noncoding RNA, Promotes Hepatocellular Carcinoma Metastasis. Hepatology 2019;70:215-230.

33. Nolan K, Walter F, Tuffy LP, Poeschel S, Gallagher R, Haunsberger S, et al. Endoplasmic reticulum stress-mediated upregulation of miR-29a enhances sensitivity to neuronal apoptosis. Eur J Neurosci 2016;43:640-652.

34. Lewis BP, Burge CB, Bartel DP. Conserved seed pairing, often flanked by adenosines, indicates that thousands of human genes are microRNA targets. Cell 2005;120:15-20.

35. **Grimson A**, **Farh KK**, Johnston WK, Garrett-Engele P, Lim LP, Bartel DP. MicroRNA targeting specificity in mammals: determinants beyond seed pairing. Mol Cell 2007;27:91-105.

36. Hotamisligil GS. Endoplasmic reticulum stress and the inflammatory basis of metabolic disease. Cell;140:900-917.

37. Febbraio MA, Reibe S, Shalapour S, Ooi GJ, Watt MJ, Karin M. Preclinical Models for Studying NASH-Driven HCC: How Useful Are They? Cell Metab 2019;29:18-26.

38. Van Herck MA, Vonghia L, Francque SM. Animal Models of Nonalcoholic Fatty Liver Disease-A Starter's Guide. Nutrients 2017;9.

39. Mendell JT, Olson EN. MicroRNAs in stress signaling and human disease. Cell 2012;148:1172-1187.

40. Bueno MJ, Gomez de Cedron M, Laresgoiti U, Fernandez-Piqueras J, Zubiaga AM, Malumbres M. Multiple E2F-induced microRNAs prevent replicative stress in response to mitogenic signaling. Mol Cell Biol 2010;30:2983-2995.

41. Byrd AE, Aragon IV, Brewer JW. MicroRNA-30c-2* limits expression of proadaptive factor XBP1 in the unfolded protein response. J Cell Biol 2012;196:689-698.

42. He Q, Li F, Li J, Li R, Zhan G, Li G, et al. MicroRNA-26a-interleukin (IL)-6-IL-17 axis regulates the development of non-alcoholic fatty liver disease in a murine model. Clin Exp Immunol 2017;187:174-184.

43. Jones MR, Quinton LJ, Blahna MT, Neilson JR, Fu S, Ivanov AR, et al. Zcchc11-dependent uridylation of microRNA directs cytokine expression. Nat Cell Biol 2009;11:1157-1163.

44. Jiang Q, Isquith J, Zipeto MA, Diep RH, Pham J, Delos Santos N, et al. Hyper-Editing of Cell-Cycle Regulatory and Tumor Suppressor RNA Promotes Malignant Progenitor Propagation. Cancer Cell 2019;35:81-94.e87.

45. Liu G, Du W, Xu H, Sun Q, Tang D, Zou S, et al. RNA G-quadruplex Regulates MicroRNA-26a Biogenesis and Function. J Hepatol 2020.

Author names in bold designate shared co-first authorship.

Figure Legends

Figure 1. MiR-26a is induced by ER stress in liver cells.

(A) Representative dot blot analysis of miR-26a in HepG2 cells treated with DMSO, tunicamycin (Tu, 2 μg/ml) or thapsigargin (Tg, 250 nM) for 24 hr. The graph on the right shows quantification of miR-26a by ImageJ.

(B) QRT-PCR analysis of miRNA expressions in HepG2 cells treated with Tu (2 μg/ml) for indicated times.

(C) HepG2 cells were treated with DMSO, Tu (2 μg/ml), Tg (250 nM) or A23187 (1 mM) for indicated times. Levels of miR-26a, miR-22, miR-29a and miR-194 were determined by QRT-PCR.

(D) miR-26a levels in Huh7 or 786-O cells treated with DMSO or Tu (2 μg/ml) for indicated times.

(E) QRT-PCR analysis of miR-26a expression in murine primary hepatocytes (MPHs) treated with Tu (2 μg/ml) or Tg (250 nM) for indicated times.

(F,G) miR-26a levels in Huh7 cells and MPHs treated with palmitate acid (PA, 300 μM) (F) or oleate acid (300 μM) (G) for indicated times.

Data are shown as mean ± SEM. **P*<0.05, ***P*<0.01, ****P*<0.001.

Figure 2. MiR-26a alleviates chemical-induced ER stress in liver cells.

(A-D) HepG2 cells were transfected with miR-26a mimics, negative control (N.C), or siRNA for eIF2α for 24 hr before the induction of ER stress, and protein and mRNA levels were determined as indicated. ImageJ quantification of the protein levels of p-eIF2α and eIF2α to actin is shown.

(A) HepG2 cells were treated with Tu (2 μg/ml) or Tg (250 nM) for 24 hr, and protein levels were determined by western blotting.

(B) Protein levels in HepG2 treated with Tu (0, 2 or 8 μg/ml) for 24 hr.

(C) Protein levels in HepG2 cells treated with Tu (2 μg/ml) for indicated times.

(D) eIF2α was knockdown by siRNA in HepG2 cells and the protein levels were determined after Tu (2 μg/ml) treatment for indicated times.

(E) mRNA levels of Bip, Chop, and Hepcidin in HepG2 cells transfected with miR-26a or N.C, followed by Tu (2 μg/ml) treatment for 5 hr.

Data are shown as mean ± SEM, **P*<0.05, ***P*<0.01, ****P*<0.001.

Figure 3. MiR-26a directly targets eIF2α.

(A) The predicted miR-26a binding sites and sequences in the 3'-UTR of human and murine Eif2s1 were analyzed by TargetScan.

(B) Relative luciferase activity in HEK293T cells co-transfected with reporter vectors containing the 3'-UTR of human Eif2s1 and co-transfected with either miR-26a or N.C. hEif2s1-1 and hEif2s1-2 vector contain four and one target sites, respectively. M, mutant. hEif2s1-1M1 or hEif2s1-M1-4, one or all four target sites were mutated in hEif2s1-1 vector. hEif2s1-2M, target site was mutated in hEif2s1-2 vector.

(C) Ago2-RIP analysis of Eif2s1 in the livers of WT and 26a DKO mice. QRT-PCR was performed to determine the mRNA levels in the Ago2 RIP fraction. Cd36 and Gapdh were used as the positive and negative control, respectively.

(D) Representative western blot analysis of eIF2α levels in HepG2, Huh7 and NHDF cells transfected with miR-26a or N.C for 24 hr (upper panel). The expressions of eIF2α to actin were quantified by ImageJ (lower panel).

(E) Representative western blot analysis of eIF2α levels in the livers of male or female Alb-TG and WT mice (upper panel). The expressions of eIF2α to actin were quantified by ImageJ (lower panel).

(F) SDS-PEAG of ^{35}S-labeled total protein. HepG2 cells were transfected with miR-26a or N.C for 24 hr, and then cultured in the media containing ^{35}S labeled methionine and with or without Tg (250 nM) for 6 hr. Actin detected by western blot was used as a loading control (left panel). Quantification of protein synthesis by ImageJ (right panel).

(G) SUnSET analysis of hepatic protein synthesis. WT and Alb-TG mice were fed a HFD for 5 days, followed by intraperitoneal injection of puromycin. Protein synthesis in mouse livers was determined by western blot for puromycin, and actin was used as a loading control (left panel). Quantification of protein synthesis was analyzed by ImageJ (right panel).

Data are shown as mean ± SEM. *P<0.05, **P<0.01, ***P<0.001.

Figure 4. Overexpression of miR-26a in mice alleviates HFD-induced ER stress.

(A-D) 6-8-week-old male Alb-TG mice and their WT littermates were fed a HFD for 16 weeks, and the indicated analyses were performed.

(A) Plasma AST and ALT levels of Alb-TG mice and their WT littermates fed a HFD (n=7-8).

(B) Representative western blot analysis of ER stress markers in the livers of in Alb-TG mice and WT littermates fed a HFD. Relative protein levels to actin were quantified by ImageJ.

(C) Expressions of Bip, Chop, and Xbp1 in the livers of Alb-TG mice and WT littermates fed a HFD (n=4).

(D) Expressions of Il-1β, Il-6, Mcp1 and Tnfα in the livers of Alb-TG mice and WT littermates fed a HFD (n=4).

(E) Protein levels in MPHs isolated from Alb-TG and WT littermates and treated with Tg (250 nM) for indicated times. Relative protein levels to actin were quantified by ImageJ.

Data are shown as mean ± SEM. **P*<0.05, ***P*<0.01, ****P*<0.001.

Figure 5. Deficiency of miR-26a aggravates chemical-induced ER stress in liver cells.

(A) Protein levels in MPHs isolated from 26a DKO mice and WT littermates and treated with Tu (2 μg/ml) for indicated times (left panel). Expressions of p-eIF2α and eIF2α to actin were quantified by ImageJ (right panel).

(B) Expressions of Bip, Chop and sXbp1 in MPHs treated with Tu (2 μg/ml) for indicated times.

(C) Protein levels in MPHs isolated from WT and 26a DKO mice and treated with Tg (250 nM) for indicated times (left panel). Expressions of p-eIF2α and eIF2α to actin were quantified by ImageJ (right panel).

(D) Expressions of Bip, Chop and sXbp1 in MPHs treated with Tg (250 nM) for indicated times.

(E) Protein levels in MPHs isolated from 26a DKO mice and transfected with Eif2s1 siRNA, followed by Tu (2 μg/ml) treatment for indicated times (left panel). ImageJ quantification of protein levels is shown (right panel).

Data are shown as mean ± SEM. **P*<0.05, ***P*<0.01, ****P*<0.001.

Figure 6. Deficiency of miR-26a in mice aggravates HFD-induced ER stress.

(A-I) 6-8-week-old male 26a DKO mice and their WT littermates were fed a HFD for 8 weeks, and the indicated analyses were performed.

(A) Body weight (n=7).

(B) Plasma ALT and AST levels (n=6-8).

(C) Representative pictures of livers from HFD-feeding mice (n=5).

(D,E) Representative Hematoxylin and Eosin (H&E) (D) and Oil red O (ORO) staining (E) of liver sections (n=5). Scale bar, 100 μm for H&E, and 50 μm for ORO.

(F) Hepatic triglyceride (TG) and total cholesterol (TC) levels (n=6-7).

(G) Plasma TG and TC levels (n=5-6).

(H) Protein levels in the livers were determined by western blot (n=3).

(I) Heat map of mRNA levels of hepatic genes involved in ER stress, lipid metabolism and inflammation. Red and blue depict higher and lower gene expression respectively. Color intensity indicates magnitude of expression differences. All listed genes were differentially expressed in two groups with significance ($p< 0.05$) (n=5-6).

Data are shown as mean ± SEM. *P<0.05, ***P<0.001.

Figure 7. MiR-26a alleviates palmitate-induced ER stress and lipid accumulation in hepatocytes.

(A) ORO staining of MPHs isolated from WT and 26a DKO mice and treated with PA (300 μM) for 24 hr. Scale bar, 100 μm.

(B) Protein levels in MPHs isolated from WT and 26a DKO mice and treated with PA for indicated times.

(C,D) Expressions of genes associated with ER stress (C) and lipid metabolism (D) in MPHs treated with PA for indicated times.

(E) MiR-26a levels in MPHs isolated from 26a DKO mice and transfected with N.C or miR-26a mimics.

(F) ORO staining of MPHs isolated from 26a DKO mice were transfected with N.C or miR-26a mimics and treated with PA for 24 hr. Scale bar, 100 μm.

(G) Protein levels in MPHs isolated from 26a DKO mice were transfected with N.C or miR-26a mimics and treated with PA for indicated times.

Data are shown as mean ± SEM. **P*<0.05, ***P*<0.01, ****P*<0.001.

Figure 8. MiR-26a was downregulated in the livers of NAFLD patients.

(A-D) Expressions of miR-26a (A), miR-26a host genes (B), primary (C) and precursor miR-26a (D) in the livers of NAFLD subjects and non-steatosis individuals were determined by QRT-PCR (n=14-18).

(E) Expressions of ER stress markers in the livers of NAFLD subjects and non-steatosis individuals (n=14-18).

(F) Protein levels of ER stress markers in the livers of NAFLD subjects and non-steatosis individuals.

(G) A schematic model of the ER stress/miR-26a feedback loop in NAFLD pathogenesis.

Data are shown as mean ± SEM. *P<0.05, **P<0.01.

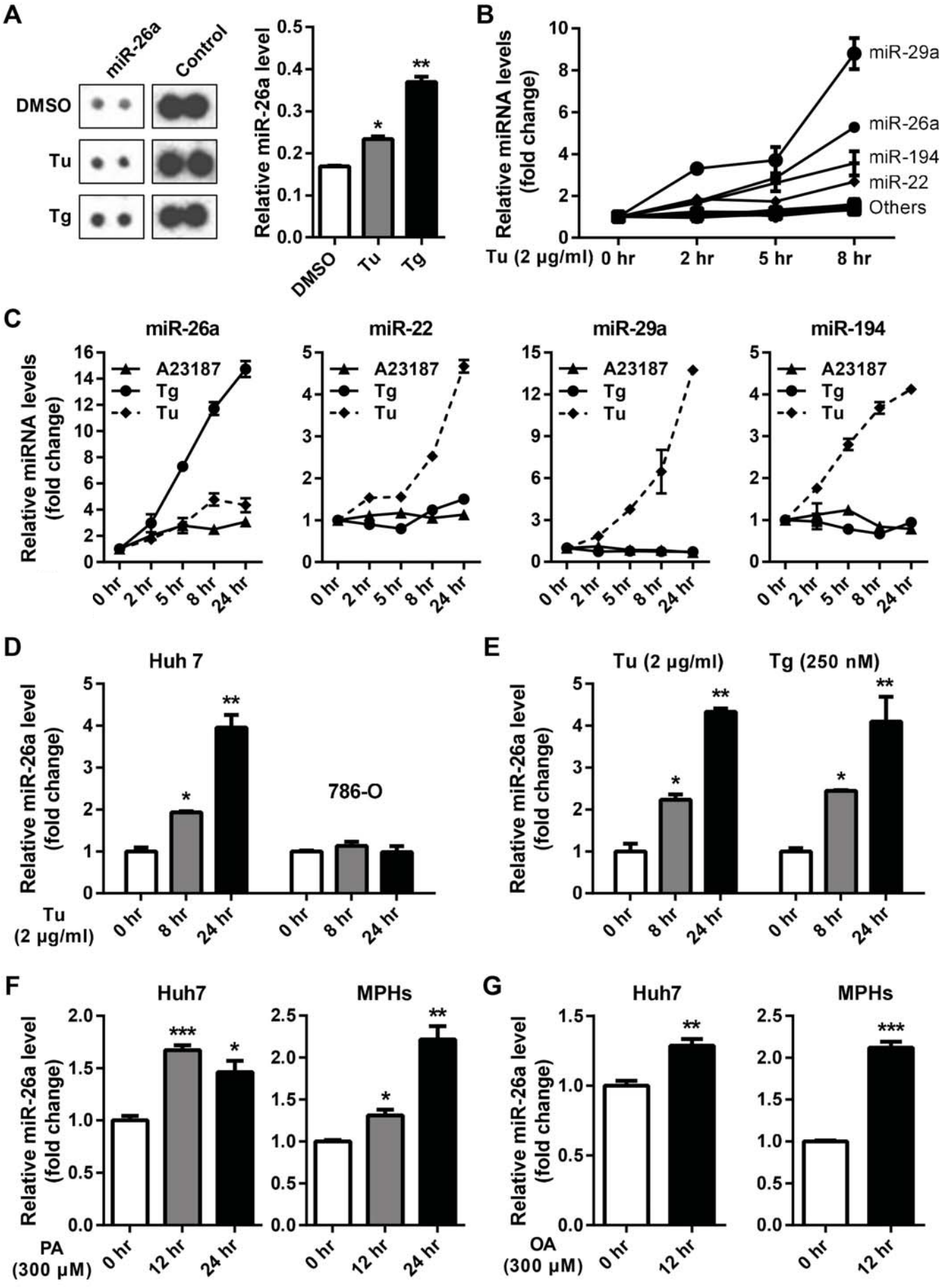
A
miR-26a
Control
DMSO
Tu
Tg
Relative miR-26a level
DMSO
Tu
Tg
B
Relative miRNA levels (fold change)
miR-29a
miR-26a
miR-194
miR-22
Others
Tu (2 μg/ml) 0 hr
2 hr
5 hr
8 hr
C
miR-26a
miR-22
miR-29a
miR-194
A23187
Tg
Tu
Relative miRNA levels (fold change)
0 hr
2 hr
5 hr
8 hr
24 hr
D
Huh 7
786-O
Relative miR-26a level (fold change)
Tu (2 μg/ml)
0 hr
8 hr
24 hr
E
Tu (2 μg/ml)
Tg (250 nM)
Relative miR-26a level (fold change)
F
Huh7
MPHs
Relative miR-26a level (fold change)
PA (300 μM)
0 hr
12 hr
24 hr
G
Huh7
MPHs
Relative miR-26a level (fold change)
OA (300 μM)
0 hr
12 hr

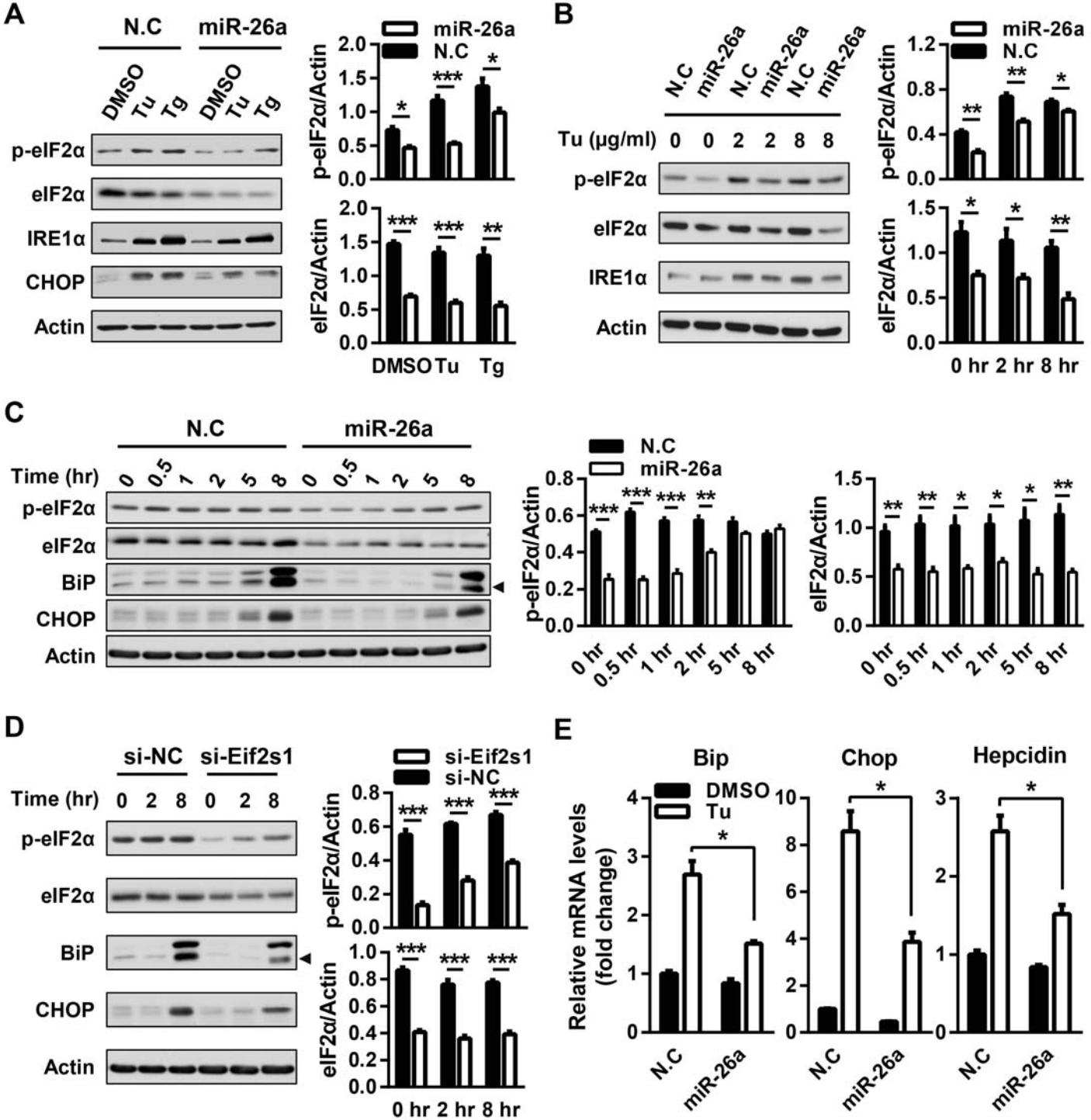
A
N.C
miR-26a
DMSO
Tu
Tg
p-eIF2α
eIF2α
IRE1α
CHOP
Actin
miR-26a
N.C
p-eIF2α/Actin
eIF2α/Actin
DMSO Tu Tg
B
Tu (μg/ml) 0 0 2 2 8 8
0 hr 2 hr 8 hr
C
Time (hr) 0 0.5 1 2 5 8
BiP
0 hr 0.5 hr 1 hr 2 hr 5 hr 8 hr
D
si-NC
si-Eif2s1
E
Bip
Chop
Hepcidin
DMSO
Tu
Relative mRNA levels (fold change)

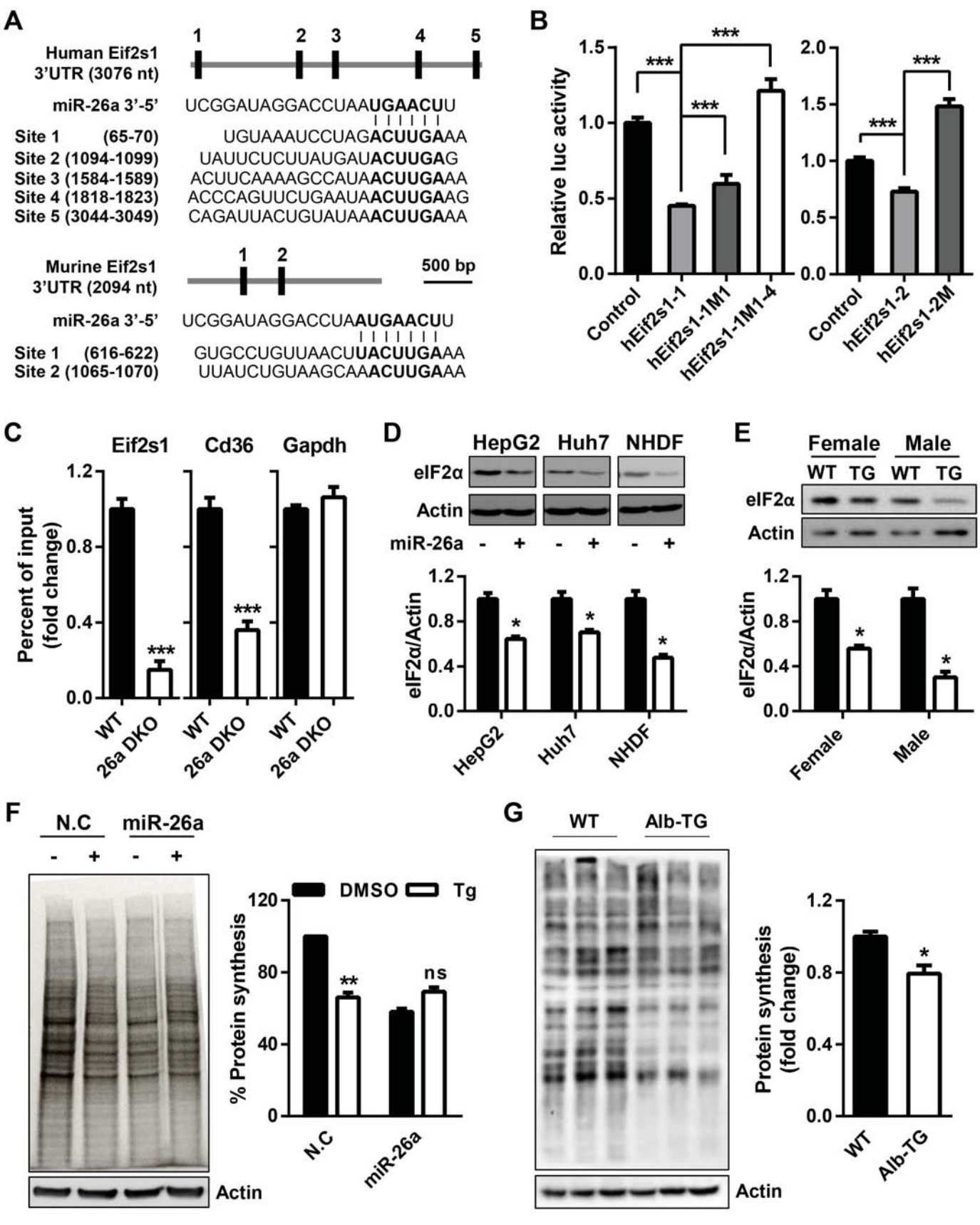
A
Human Eif2s1
3'UTR (3076 nt)
1 2 3 4 5
miR-26a 3'-5' UCGGAUAGGACCUAAUGAACUU
Site 1 (65-70) UGUAAAUCCUAGACUUGAAA
Site 2 (1094-1099) UAUUCUCUUAUGAUACUUGAG
Site 3 (1584-1589) ACUUCAAAAGCCAUAACUUGAAA
Site 4 (1818-1823) ACCCAGUUCUGAAUAACUUGAAG
Site 5 (3044-3049) CAGAUUACUGUAUAAACUUGAAA
Murine Eif2s1
3'UTR (2094 nt)
1 2
500 bp
miR-26a 3'-5' UCGGAUAGGACCUAAUGAACUU
Site 1 (616-622) GUGCCUGUUAACUUACUUGAAA
Site 2 (1065-1070) UUAUCUGUAAGCAACUUGAAA
B
Relative luc activity
***
Control
hEif2s1-1
hEif2s1-1M1
hEif2s1-1M1-4
hEif2s1-2
hEif2s1-2M
C
Eif2s1
Cd36
Gapdh
Percent of input (fold change)
WT
26a DKO
D
HepG2
Huh7
NHDF
eIF2α
Actin
miR-26a
eIF2α/Actin
E
Female
Male
WT
TG
F
N.C
miR-26a
DMSO
Tg
% Protein synthesis
ns
G
WT
Alb-TG
Protein synthesis (fold change)

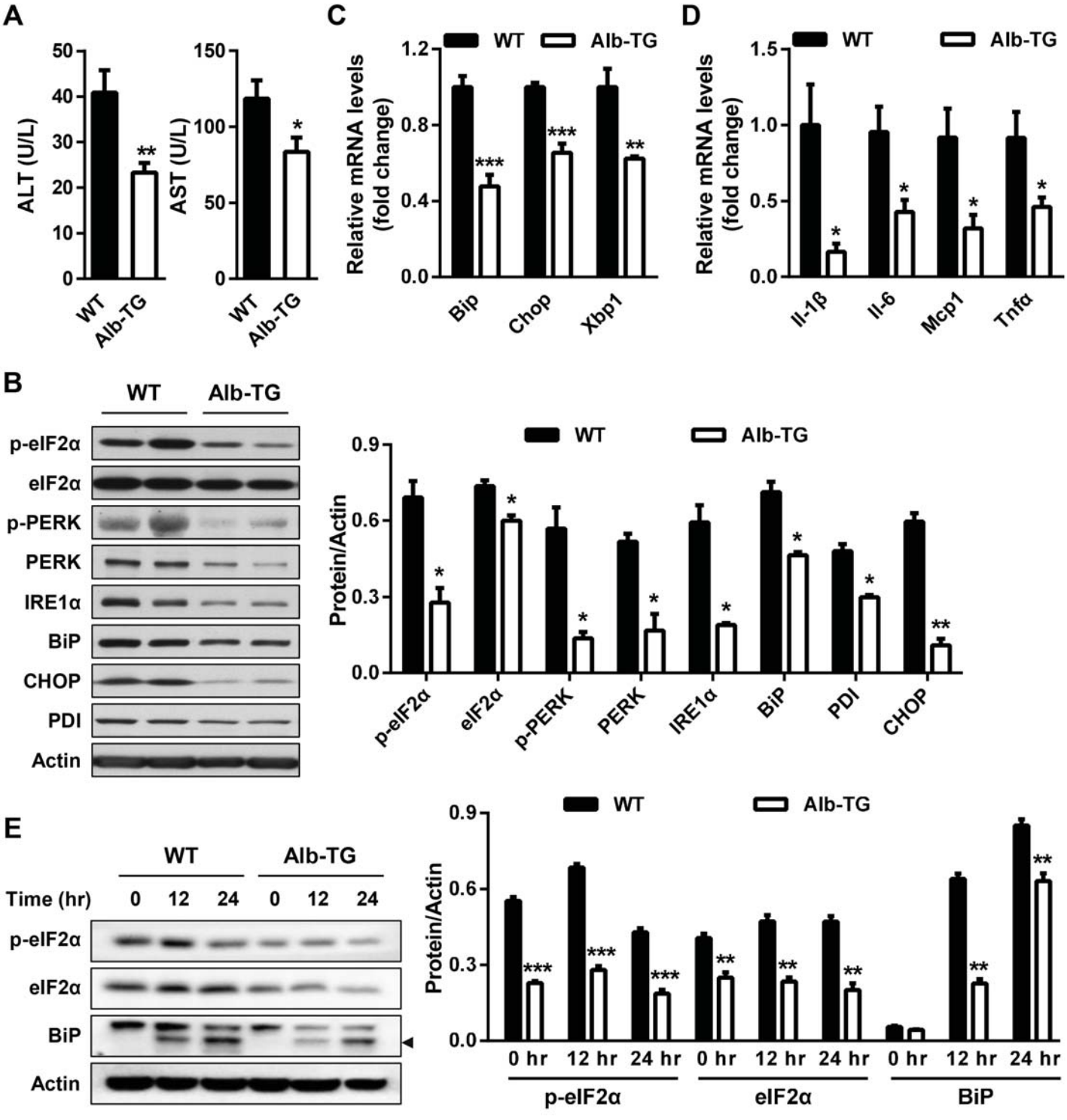
A
ALT (U/L)
AST (U/L)
WT
Alb-TG
C
Relative mRNA levels (fold change)
Bip
Chop
Xbp1
D
Il-1β
Il-6
Mcp1
Tnfα
B
p-eIF2α
eIF2α
p-PERK
PERK
IRE1α
BiP
CHOP
PDI
Actin
Protein/Actin
E
Time (hr)
0
12
24
0 hr
12 hr
24 hr

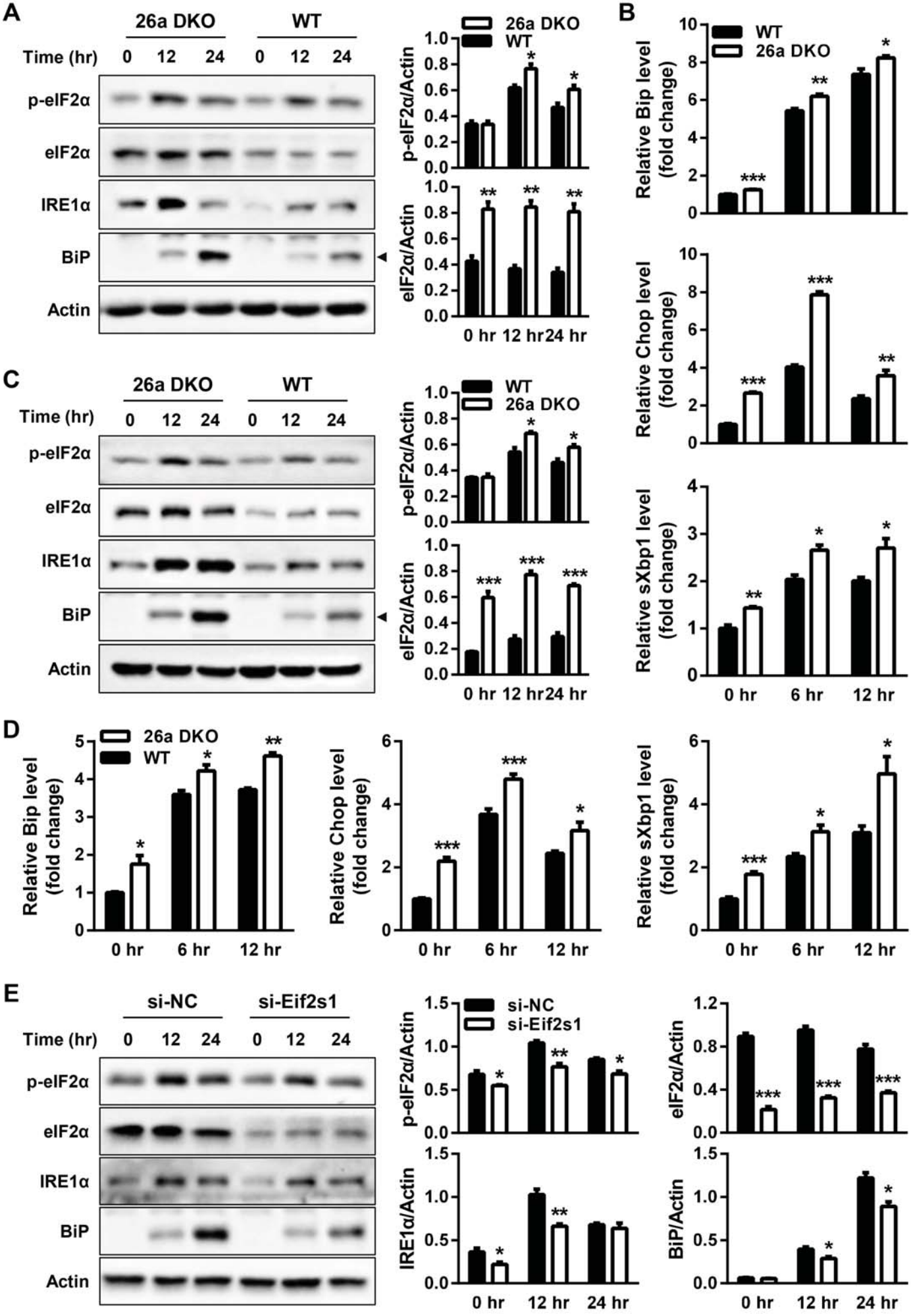
A
26a DKO
WT
Time (hr)
0 12 24 0 12 24
p-eIF2α
eIF2α
IRE1α
BiP
Actin
26a DKO
WT
p-eIF2α/Actin
eIF2α/Actin
0 hr 12 hr 24 hr
B
WT
26a DKO
Relative Bip level (fold change)
Relative Chop level (fold change)
Relative sXbp1 level (fold change)
0 hr 6 hr 12 hr
C
26a DKO
WT
Time (hr)
0 12 24 0 12 24
p-eIF2α
eIF2α
IRE1α
BiP
Actin
WT
26a DKO
p-eIF2α/Actin
eIF2α/Actin
0 hr 12 hr 24 hr
D
26a DKO
WT
Relative Bip level (fold change)
Relative Chop level (fold change)
Relative sXbp1 level (fold change)
0 hr 6 hr 12 hr
E
si-NC
si-Eif2s1
Time (hr)
0 12 24 0 12 24
p-eIF2α
eIF2α
IRE1α
BiP
Actin
si-NC
si-Eif2s1
p-eIF2α/Actin
eIF2α/Actin
IRE1α/Actin
BiP/Actin
0 hr 12 hr 24 hr

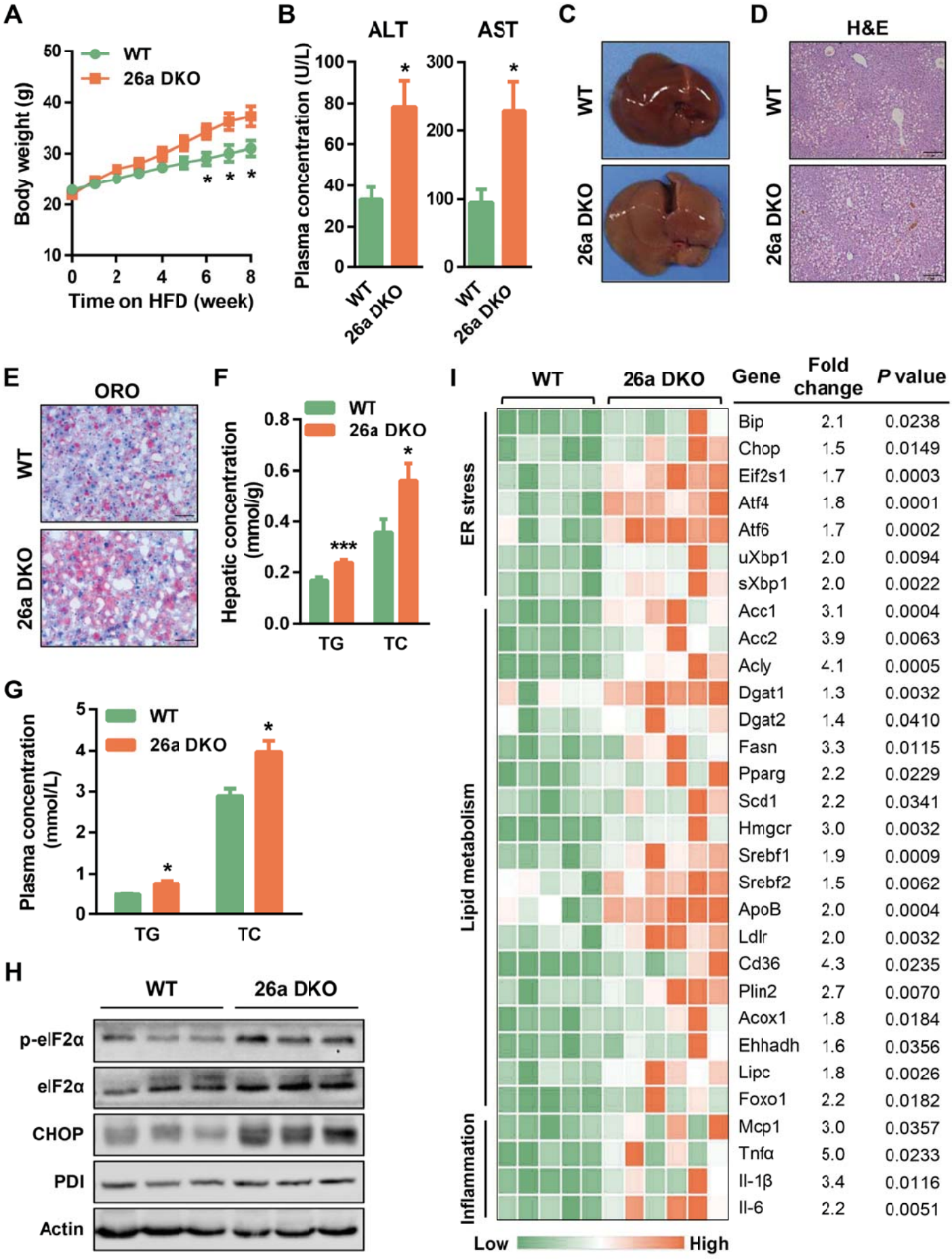

Gene	Fold change	*P* value
Bip	2.1	0.0238
Chop	1.5	0.0149
Eif2s1	1.7	0.0003
Atf4	1.8	0.0001
Atf6	1.7	0.0002
uXbp1	2.0	0.0094
sXbp1	2.0	0.0022
Acc1	3.1	0.0004
Acc2	3.9	0.0063
Acly	4.1	0.0005
Dgat1	1.3	0.0032
Dgat2	1.4	0.0410
Fasn	3.3	0.0115
Pparg	2.2	0.0229
Scd1	2.2	0.0341
Hmgcr	3.0	0.0032
Srebf1	1.9	0.0009
Srebf2	1.5	0.0062
ApoB	2.0	0.0004
Ldlr	2.0	0.0032
Cd36	4.3	0.0235
Plin2	2.7	0.0070
Acox1	1.8	0.0184
Ehhadh	1.6	0.0356
Lipc	1.8	0.0026
Foxo1	2.2	0.0182
Mcp1	3.0	0.0357
Tnfα	5.0	0.0233
Il-1β	3.4	0.0116
Il-6	2.2	0.0051

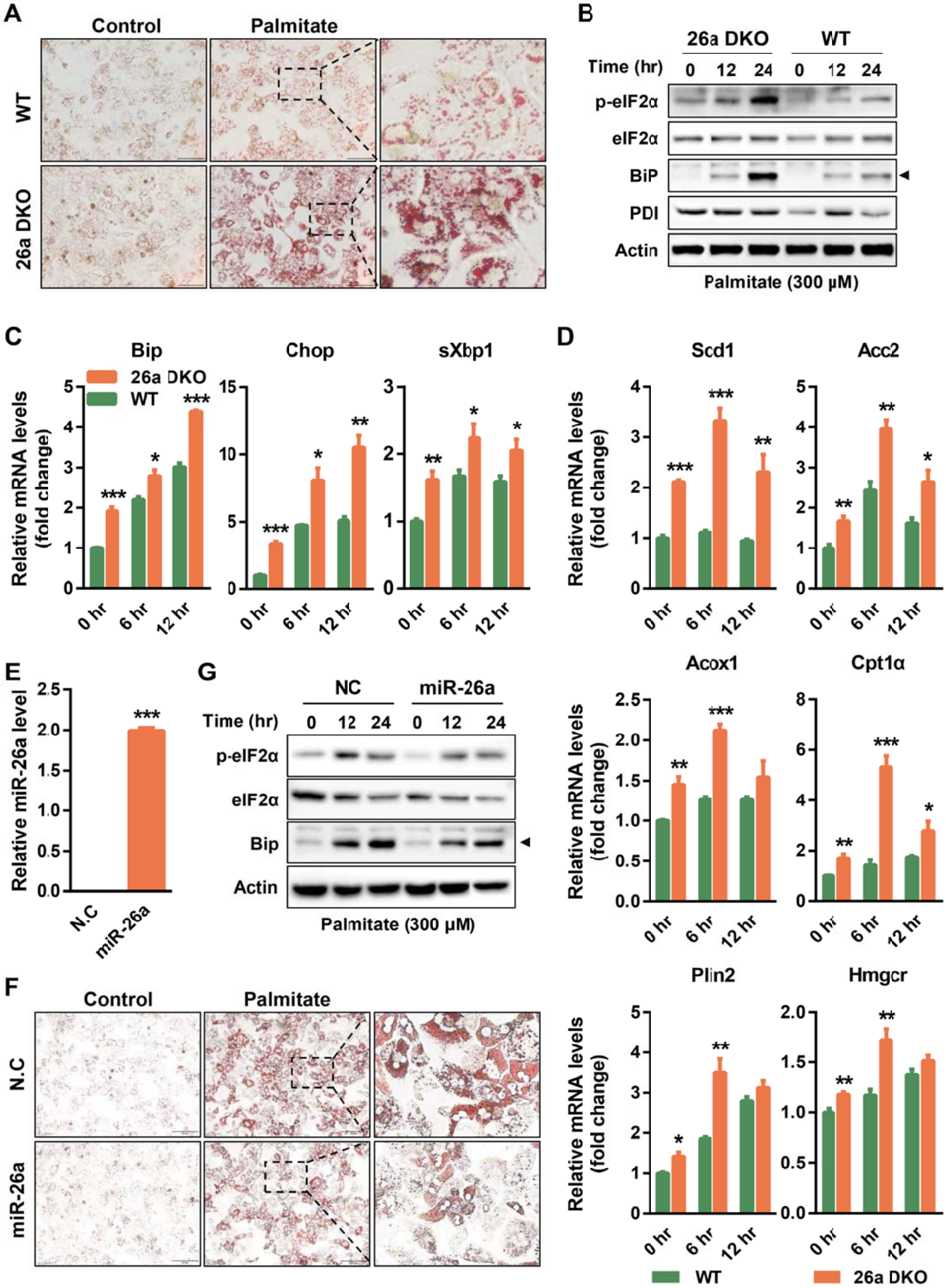
A
Control
Palmitate
WT
26a DKO
B
26a DKO
WT
Time (hr)
0 12 24 0 12 24
p-eIF2α
eIF2α
BiP
PDI
Actin
Palmitate (300 μM)
C
Bip
Chop
sXbp1
26a DKO
WT
Relative mRNA levels (fold change)
0 hr
6 hr
12 hr
D
Scd1
Acc2
Acox1
Cpt1α
Plin2
Hmgcr
Relative mRNA levels (fold change)
WT
26a DKO
E
Relative miR-26a level
N.C
miR-26a
G
NC
miR-26a
Time (hr)
0 12 24 0 12 24
p-eIF2α
eIF2α
Bip
Actin
Palmitate (300 μM)
F
Control
Palmitate
N.C
miR-26a

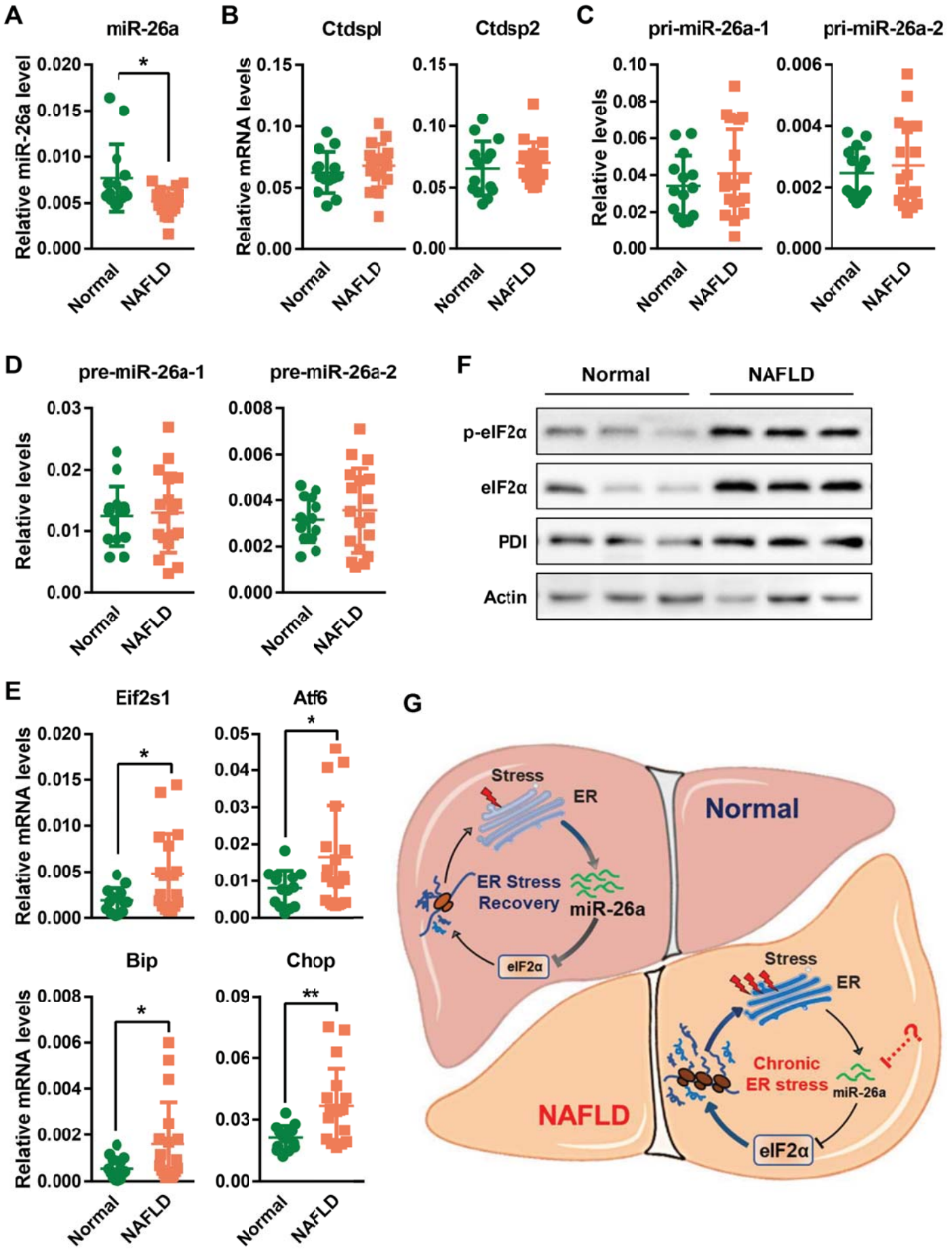
A
miR-26a
Relative miR-26a level
0.020
0.015
0.010
0.005
0.000
*
Normal
NAFLD
B
Ctdspl
Ctdsp2
Relative mRNA levels
0.15
0.10
0.05
0.00
Normal
NAFLD
C
pri-miR-26a-1
pri-miR-26a-2
Relative levels
0.10
0.08
0.06
0.04
0.02
0.00
0.006
0.004
0.002
0.000
Normal
NAFLD
D
pre-miR-26a-1
pre-miR-26a-2
Relative levels
0.03
0.02
0.01
0.00
0.008
0.006
0.004
0.002
0.000
Normal
NAFLD
F
Normal
NAFLD
p-eIF2α
eIF2α
PDI
Actin
E
Eif2s1
Atf6
Bip
Chop
Relative mRNA levels
0.020
0.015
0.010
0.005
0.000
0.05
0.04
0.03
0.02
0.01
0.00
0.008
0.006
0.004
0.002
0.000
0.09
0.06
0.03
0.00
*
**
Normal
NAFLD
G
Stress
ER
Normal
ER Stress
Recovery
miR-26a
eIF2α
Stress
ER
Chronic
ER stress
miR-26a
NAFLD
eIF2α